

Examples of Fatigue Lifetime and Reliability Evaluation of Larger Wind Turbine Components

Niels Jacob Tarp-Johansen

Abstract

This report is one out of several that constitute the final report on the ELSAM funded PSO project “Vindmøllekomponenters udmattelsesstyrke og levetid”, project no. 2079, which regards the lifetime distribution of larger wind turbine components in a generic turbine that has real life dimensions.

Though it was the initial intention of the project to consider only the distribution of lifetimes the work reported in this document provides also calculations of reliabilities and partial load safety factors under specific assumptions about uncertainty sources, as reliabilities are considered to be of general interest to potential readers too.

ISBN 87-550-3236-2 (Internet)
ISSN 0106-2840

Contents

Introduction	5
1 The Approach Taken	7
1.1 Project Limitations	7
1.2 Lifetime Distributions and Reliability	8
1.3 The Steps to Obtain the Lifetime Distribution	8
1.4 Sources of Uncertainty	10
1.4.1 Remark on Gross Errors	12
1.5 Numerical Scheme	12
2 Lifetime Evaluation	13
2.1 Limit-State Function	13
2.1.1 Bin-Wise Expected Lifetimes	16
2.2 Stochastic Model	19
2.2.1 Statistical Uncertainty of Mean Wind Distribution	19
2.2.2 Inherent and Statistical Uncertainty of Material Data	20
2.2.3 Model Uncertainties	25
2.3 Results	26
3 Reliability Considerations	33
3.1 The Calibration Procedure	33
3.2 Results	35
4 Conclusions	39
References	41

Introduction

This report is one out of several that constitute the final report on the project ELSAM funded PSO project “Vindmøllekomponenters udmattelsesstyrke og levetid”, project no. 2079, which regards the lifetime distribution of larger wind turbine components in a generic turbine that has real life dimensions.

In the present report the probabilistic part of the project is given. In other parts of the project the following has been treated:

- Material properties of the three types of steel used for the three components (hub, main shaft, and main frame) that has been considered in the project, i.e. determination of SN-curves
- Design of the components to fit into the generic turbine followed by determination of transfer function from cross-sectional loads to hot-spot stresses
- Simulation of wind turbine response at given mean wind speeds, and subsequently assessment of lifetimes of the components conditional on the considered mean wind speeds

Based on this input this report evaluates the lifetime distributions of the components. Actually, it was the initial intention of the project to consider only the distribution of lifetimes however, as the distribution of lifetimes and the reliability are directly connected, the work reported in this document provides also calculations of reliabilities and partial load safety factors under specific assumptions about uncertainty sources, as reliabilities are considered to be of general interest to potential readers too.

The study in this report constitutes a simplified probabilistic analysis where some short cuts are made here and there. In the report it is attempted to provide comments on the deviations made from a more complete approach. Some of the results and conclusions reached in this report are – in the author’s mind – however considered to be of general qualitative validity, though they are expected to deviate quantitatively from those obtained if a more detailed analysis had been conducted.

One of the notable conclusions is that the reliability differs considerably among the components. This can be explained by the fact that three different manufacturers have contributed each with one of the components. The differences are therefore expected to result partly from the fact that different manufacturers may have different design strategies, partly from the fact that in any turbine not all components are designed fully to the limit. Thus any turbine design has a bottleneck, which then can be one of the components considered herein.

The project originally contained a demonstration/verification task that had the aim of comparing experimental results to the results coming out of the work covered in the present report. This task was cancelled at an early stage of the project, when the current project team took over the project from the initiating project team, as the author of this report found it impossible – or at least very difficult – to carry out such experiments that would be needed to verify the theoretical results obtained in the project. The experiments would have to prove that the obtained lifetime distributions were correct. As it becomes apparent in

the report the lifetimes are in the range of ten to thousand years, results that certainly support the decision made. Because the project considers components from real-life structures that are naturally designed with the aim of very few collapses such results are not unrealistic. Therefore the project team is confident that the right decision was made. Moreover, to a large extent, the lifetime distribution depends on many other uncertainties than the natural randomness of material properties. Implying that experiments should be constructed such that these uncertainties could be accounted for as well. Because these uncertainties are model uncertainties this can hardly be done. The conclusion gives recommendations on what should be done instead.

The report is divided into three chapters contains:

1. The theoretical approach behind the probabilistic evaluation
2. Calculations leading to the lifetime distributions
3. Discussions of reliabilities and partial safety factors.

Some of the material given in this report is an extension of the note [1] that the author complied at an early stage of the project. The note deals with a simulation approach to the numerics behind the probabilistic results. As discussed in Chapter 1 the method has turned out to be inapplicable.

1 The Approach Taken

Equation Chapter 1 Section 1 This chapter describes the approach and modelling employed in this work to assess the lifetime distributions and reliabilities. Essentially the approach consists in pinning out the possible sources on randomness and uncertainty that contribute to the lifetime distribution and then trying to assess the distributions of the uncertainties. Finally one applies a suitable numerical scheme to assess the distribution of the lifetime and the reliabilities.

1.1 Project Limitations

Up to now lifetime distribution and reliability have been mentioned without going into detail. This section provides a clarification of what will be considered in this work. A probabilistic approach is required because not only are the components subjected to fluctuating loads with a substantial random content and only does the material properties exhibit inherent variability which can be properly modelled by use of random variables, but also because considerable statistical uncertainty and so-called model uncertainties enter into the lifetime assessment.

A number of relevant probabilistic problems relate to the assessment of lifetimes for structural components subjected to fatigue loads. Among these are:

1. Determination of the lifetime distribution taking into account all of the relevant uncertainty sources
2. Determination of design such that the probability of rupture within a given design lifetime requirement becomes sufficiently small
3. Determination of partial safety factors that approximately lead to 2
4. Determination of optimal inspection planning such that the same probability of rupture is obtained with lesser dimensions without inspection costs becoming unacceptably high.

These problems are more or less sophisticated variations over the same theme. Central to all of these problems is the examination of the uncertainties that cannot be classified as inherent or natural. Ideally the lifetime distribution depends on the natural variation of the external loads and the natural variation of the fatigue resistance among material specimens. Because the external load that leads to the fatigue does not consist in a single contribution but rather in the average of a sum of many contributions the variation of the lifetime – if everything else is kept constant – is practically negligible. The inherent variation of material properties has a much larger impact on the variation of the lifetime distribution. Now, statistical uncertainties, which can always be given a probabilistic interpretation, related to the estimation of the SN-curve may potentially have an even larger impact on the uncertainty of the lifetime, i.e. on the lifetime distribution. Note that over the past few sentences the concept of lifetime distribution has shifted from what one would intuitively understand as the actual lifetime distribution to the understanding that will prevail throughout the remainder of this report, namely: the lifetime distribution embraces also the uncertainties that

are not of ‘inherent randomness’ nature. This may seem contra-intuitive to some, however from a rational point of view the latter understanding is to be preferred. Say an engineer is asked to give a statement about the probability that a certain component will survive a given fatigue load history over N years she faces the fact that, if she could gather rupture data from components that had the same design and had been subjected to the same load history, the lifetimes would show a larger scatter than should be expected from an evaluation based purely on natural randomness. The scattered data would however still appear as the outcome of a random experiment. Thus including the statistical uncertainty in the lifetime distribution is definitely meaningful. Following this line of reasoning including also the model uncertainties related e.g. to the modelling of the aerodynamic loads in the lifetime distribution should also be done. A further discussion of the different uncertainty sources is given in Section 1.4.

The work presented herein is limited to point 1 and 3, but it is not limited to the natural randomness only, on the contrary other uncertainty sources are considered at least as important – if not more important – to the fatigue life/reliability.

1.2 Lifetime Distributions and Reliability

Before proceeding it is convenient to establish the straightforward link between lifetime distributions and reliabilities. The lifetime distribution function F is defined by

$$F(l) = \Pr\{L \leq l\} \quad (1.1)$$

where L denotes the random variable for the lifetime and ‘Pr’ stands for probability. On the other hand the reliability R is defined by

$$\begin{aligned} R &= 1 - \Pr\{\text{The component ruptures due to fatigue}\} \\ &= 1 - \Pr\{L \leq l_{\text{design lifetime}}\} \\ &= 1 - F(l_{\text{design lifetime}}) \end{aligned} \quad (1.2)$$

The aimed design lifetime $l_{\text{design lifetime}}$ is for instance 20 or 50 years. In the remainder of the report $\Pr\{\text{The component ruptures due to fatigue}\}$ will for short be referred to as the probability of failure p_f or simply the failure probability.

It is the probability of failure that is evaluated by the numerical scheme described below. Thus, to interpret the results coming out of the numerics we need the relations

$$\begin{aligned} F(l) &= p_f(l) \\ R(l_{\text{design lifetime}}) &= 1 - p_f(l_{\text{design lifetime}}) \end{aligned} \quad (1.3)$$

which show the simple interconnection between the reliability and lifetime distribution.

1.3 The Steps to Obtain the Lifetime Distribution

It is further helpful for the subsequent presentation to briefly recapitulate the procedure to follow to obtain the fatigue lifetime. For clarity all other uncertain-

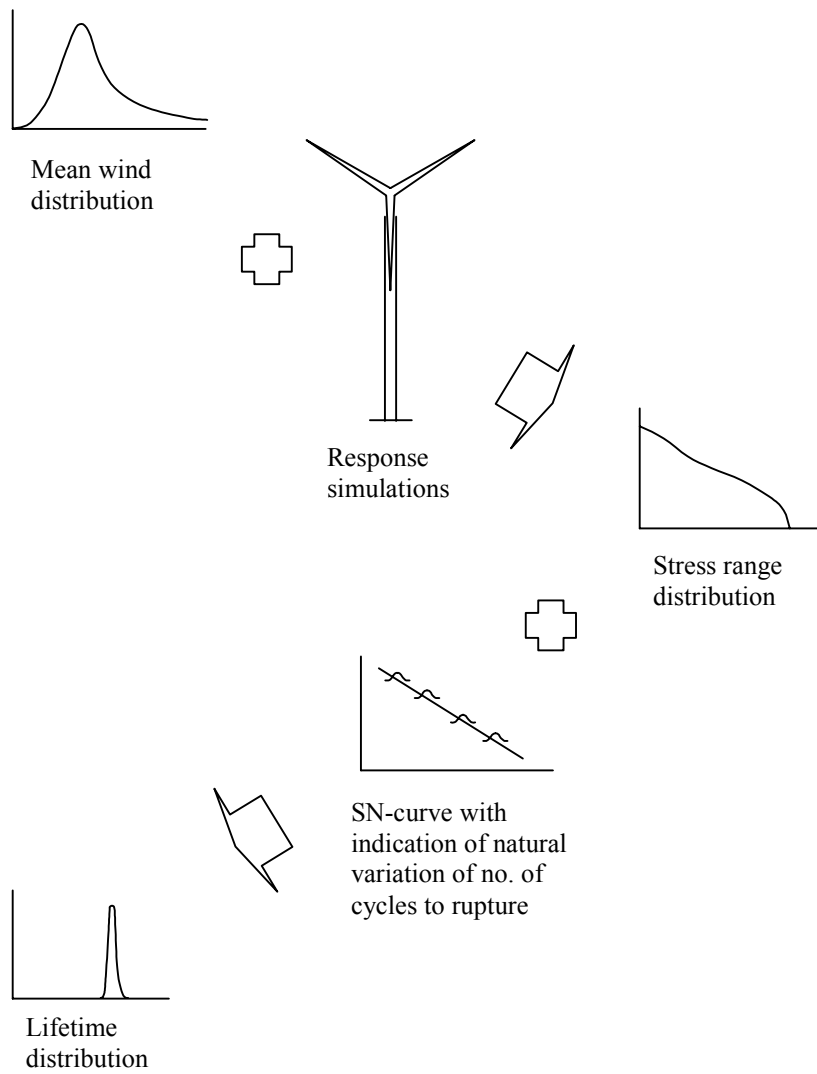


Figure 1: from mean wind distribution to lifetime distribution.

ties than natural randomness are neglected in this section. In Section 1.4 the neglected uncertainties are discussed with reference to their introduction into the procedure.

Figure 1 shows a schematic of the procedure. The starting point is the mean wind distribution and turbulence intensity distribution plus, which is not shown, assumptions about yaw errors and other possible operational modes that will contribute to the lifetime consumption. In the present work a rather simple load history without faults, start-ups and shutdowns is considered. Likewise the turbulence intensity distribution is also neglected, the latter being of less importance due to the averaging inherent in fatigue. Typically FEM time domain simulations involving aerodynamic models obtain next response time series conditional on mean wind. The third step is to establish the stress range distribution by combining the mean wind distribution and the conditional response from step two which has been subject to a more or less advanced stress range count. It is in this third step the inherent fluctuations among realisations of the turbulent wind field, even for given mean wind and turbulence intensity, appear. These fluctuations are, as already mentioned negligible. So are the fluctuations

due to variations between realisations of the mean wind distribution that has implicitly been assumed zero in this procedure. The fourth step is the Wöhler curve with modelling of the natural randomness of material properties leading to some distribution around the SN-curve of the number of cycles to rupture. It is this distribution that contributes the most to the lifetime distribution that is finally obtained in the fifth step where the distribution of cycles to rupture conditional on stress range is convolved with the stress range distribution.

1.4 Sources of Uncertainty

In this section an attempt is made at providing an exhaustive list of the various sources of uncertainties that influences the lifetime distribution. The idea is to follow the path laid out in Figure 1. At each step the possible uncertainty inputs are then discussed. Preferably the inputs would then also be quantified in terms of distributions, however during the course of the project it has shown difficult to either obtain useful data to substantiate specific choices of distributions, or to arrive at consensus about an expert judgement of the distributions. These are therefore to be assessed in another project, while in this work sort of sensitivity studies are conducted in order to guide future decision-making regarding choices of distributions. In subsections 2.2.1, 2.2.2 and 2.2.3, though, one will find some discussions concerning material uncertainties and model uncertainties relating to evaluation of aerodynamic loads. As will be apparent from the discussion below the minute one starts to think about uncertainty sources related to the response simulation, the stress range count, and the application of the SN-curve, the picture becomes so full of details that it seems that the only feasible approach is to assess the overall uncertainty of the lifetime by inviting different engineers to compute the lifetime of a certain specimen, that is not described in a standard. The different results that would come out of these computations would then account for the distribution of the lifetime uncertainty due to the uncertainties related to the response simulation, the stress range count, and the application of the SN-curve.

Mean Wind Distribution

The mean wind distribution at a given site may be estimated from one year of measurements or taken from a standard or e.g. estimated from a WASP analysis. In the first case uncertainties in terms of statistical uncertainties appear because one year of measurements cannot contain the same amount of information about the mean wind distribution as for instance 50 years, see Section 2.2.1. In the second case model uncertainties are introduced, whereas in the latter both model and statistical uncertainties mix.

Response Simulations

Unless clearly stated below all uncertainties are of model uncertainty type. There are two steps in the response calculation

1. Simulation of the dynamics of the turbine
2. Detailed analysis (typically FEM) of the considered component

Regarding the first step the uncertainties relate to

- Modelling of the upstream airflow
- Modelling of the aerodynamic loads
- Modelling of turbine's structural properties

This list could have been made more detailed, however the focus has been more on understanding the second step. In order to cut a long story short merely a list of possible sources concerning step two is stated. Essentially the uncertainties

relate to: 1) bringing reality into a manageable mechanical model, 2) bringing the mechanical model into a computational model, and 3) the engineer's interpretation of results.

Geometry (from reality to mechanical model)

1. Mismatch between drawings and FE model. Specifications may change without FE model being updated. Such an error is to be considered a gross error and not a true uncertainty source see Sec. 1.4.1.
2. Mismatch between drawings and fabrication. As long as tolerances are kept, this source qualifies as a true uncertainty source.

Boundary conditions (from reality to mechanical model)

1. Simplification of clamping, e.g. replacing a flexible joint by a rigid
2. Simplification of stress distribution, e.g. along interface between blade and hub.

Transfer functions

1. Neglecting welds (from reality to mechanical model)
2. Mesh generation and shape function choice influences stress concentration (from mechanical to computational model)
3. The user can make small errors, because she does not fully understand how iterations and hysteresis are defined in the applied FE program (interpretation of results)

Selection of hotspots

1. Selection based on engineering judgement: e.g. the points of max von Mises stress in extreme load computations or at critical design details (this source is actually closer to being a potential source of gross errors)
2. Selection on the basis of a number of load cases leading to different ratios of the stresses.
3. In both cases an assumption of linear transfer from loads to stresses.

Stress range count

A unique stress count algorithm does not exist. The rain flow count (RFC) scheme seems to be generally accepted as the method that provides the most meaningful stress range distribution for metallic materials. Since RFC is widely used a minor contribution to model uncertainties from stress range counting can be expected. Some statistical uncertainty is of course also arising from range counting of a limited number of simulated response time series.

SN-curve

The modelling of the SN-curve contributes mainly to model uncertainties. However some statistical uncertainty also originates from the fact that SN-curves are sometimes estimated by linear regression based on a limited number of tests. The following issues are expected to contribute to the uncertainty

1. General
 - a. The approximate validity of Miner's rule
 - b. The influence of mean stresses
 - c. Extrapolation of SN-curves to small stress ranges
2. Synthetic SN-curves
 - a. The general nature of synthetic SN-curves taken from standards
 - b. Erroneous choice of synthetic SN-curve (gross-error-category)
3. SN-curves based on tests
 - a. Tests are conducted on specimens, not on full-scale components
 - b. Deviation of test data from a straight line
 - c. Estimation of an SN-curve from a limited number of data

1.4.1 Remark on Gross Errors

As the reader may have noticed some of the uncertainty sources listed above has actually been categorised as gross errors. They have been included in the list with the purpose of putting the discussion of uncertainties into perspective.

Partial safety factors are not intended to provide safety against gross errors (like omitting a bar in a latticed structure) that should be captured by the quality control. Aiming at developing safety factors for gross errors too would end up in uneconomic design.

The author expects that despite of quality control there is a non-negligible risk that some gross errors will remain. Especially a critical issue is the selection of hot spots, which is a difficult discipline. At present, i.e. with the current rules of design, the author estimates, that the extra uncertainty due to such a hot spot error is countered by the conservative assessment of the characteristic fatigue loads. This being of course an irrational design situation that ought to be further investigated.

1.5 Numerical Scheme

It was the initially the intention of the project to apply a simulation technique to assess the probability distribution of the lifetimes. However the probabilities, i.e. the failure probabilities, that are of interest in the current project are very small, i.e. in the range from 10^{-8} to 10^{-4} . These small probabilities reflect the fact that the project considers component from real live structures that are designed with the aim of very few collapses, i.e. long expected lifetimes. Simulation techniques require that the events that contribute to the probability which one wants to estimate occur several times among the simulation results. Otherwise stable estimates of the probability wanted are not obtained. Consequently, if one seeks probabilities in the range mentioned, the number of simulations needed would be in the range from 10^6 to 10^{10} . A simulation procedure that was developed during the course of the project is described in the note [1]. Though the procedure aims at being cheap in terms of computer time per simulation loop it is still impractical to apply such a method in the current context. Therefore the simulation approach has been abandoned in favour of a more sophisticated numerical procedure – the so-called First Order Reliability Method (in short: FORM), which is extensively described in e.g. [2]. The FORM procedure computes directly the probability of failure p_f required in formulas (1.3).

2 Lifetime Evaluation

Equation Chapter (Next) Section 1 This chapter is the core part of the report as the employed limit-state function and stochastic model are described; including some suggestions for, and some examples of, quantification of model uncertainties. Further several examples of lifetime distributions are given.

2.1 Limit-State Function

In the context of structural reliability, which is the context of this work, the stochastic model is the specification of the distributions of the stochastic variables that enter into the problem under consideration. Recalling what was shown in Section 1.2, the problem is finding the probability that some structural failure event occurs; that is finding the probability that the component is subjected to loads that brings the component into a failure mode, i.e. a mode on the unfortunate side of the limit between safe and unsafe modes. To the end of distinguishing safe modes from unsafe modes the so-called limit-state function $g(\mathbf{X}) = g(X_1, X_2, \dots, X_n)$ is defined. The quantity \mathbf{X} denotes the vector of random variables that enter the problem, i.e. material strengths, loads, and model uncertainties. The limit-state function shall be defined such that it takes positive values when the random variables take values that correspond to the component being in a safe mode; that is if the strength variables take high values and load variables take low values. On the other hand, if the random variables take values that correspond to component rupture the limit-state function shall take negative values. Finally the limit-state function is zero for any combination of the random variables that neither is a safe mode nor a rupture mode, i.e. modes just on the edge of rupture – thereby the name “limit-state function”. Having defined $g(\bullet)$ evaluating the probability of failure therefore boils down to

$$\begin{aligned} \Pr\{\text{failure}\} &= \Pr\{g(\mathbf{X}) \leq 0\} \\ &= \Pr\{g(X_1, X_2, \dots, X_n) \leq 0\} \end{aligned} \tag{2.1}$$

So stating the stochastic model requires also stating the limit-state function. In the following the limit-state function is developed. Then, in the next section the stochastic model follows.

Start out disregarding the model uncertainties. By use of a discretised Miner's rule the probability of failure is given by

$$p_f = \Pr\{L \leq l\} = \Pr\left\{\sum_i \frac{n_i l}{N_i} \geq 1\right\} \tag{2.2}$$

where n_i is the frequency (number per unit time) of cycles at stress range level σ_i , and N_i is the number of cycles to rupture at the stress range level σ_i . According to the SN-curve model N_i is given by $N_i = \varepsilon^{\frac{1}{2}} (\sigma_i / \sigma')^{-m}$ (except for

the ε , the notation follows the one defined in [5]). The random variable ε , which has mean 1, accounts for the random spread of number of cycles to rupture around the SN-curve. Thus the limit-state function becomes

$$g(n_i, m, \sigma', \varepsilon) = 1 - \sum_i \frac{n_i l}{\varepsilon^{\frac{1}{2}} (\sigma_i / \sigma')^{-m}} \quad (2.3)$$

Note that n_i has been included in the list of arguments to $g(\cdot)$ because, strictly speaking it is a random variable, though its variation is practically negligible. In the following this variation is neglected, and instead the statistical uncertainty of the mean wind distribution is accounted for by randomness of n_i . The variables m and σ' are assigned distributions that account for the statistical uncertainties related to the estimation of the SN-curve from data. In order to make the limit-state function work with results obtained prior in the project it has to be reformulated. Later it will become clear that this reformulation puts some limits on the generality of the results. Because all mean wind speeds contribute to the stress range σ_i formula (2.3) can be rewritten into

$$g(p_j, m, \sigma', \varepsilon) = 1 - \sum_j p_j l \sum_i \frac{n_{ij}}{\varepsilon^{\frac{1}{2}} (\sigma_i / \sigma')^{-m}} \quad (2.4)$$

where p_j is the probability of the 10-min. mean wind speed bin $U_{10,j}$, and n_{ij} is the frequency of cycles at stress range level σ_i and 10-min. mean wind speed $U_{10,j}$. In essence n_i has been substituted by the product $p_j n_{ij}$ where p_j will account uncertainty of the mean wind distribution and the fact that the inherent randomness of n_i is neglected render n_{ij} a deterministic variable. Denoting by l_j the expected lifetime of a component subjected only to loads derived from mean wind speed bin j , i.e.

$$l_j(m, \sigma') = \frac{1}{\sum_i \frac{n_{ij}}{\varepsilon^{\frac{1}{2}} (\sigma_i / \sigma')^{-m}}} \quad (2.5)$$

the formula (2.4) simplifies to

$$g(p_j, m, \sigma', \varepsilon) = 1 - \sum_j \frac{p_j l_j}{\varepsilon l_j(m, \sigma')} \quad (2.6)$$

It follows from formula (2.5) that for given m and σ' the l_j 's can be computed directly from a stress range count at each mean wind speed. In this way the complexity of the input to the limit-state function is reduced from the stress range distributions to the expected lifetimes conditional on mean wind speed. The reduction is obtained at the expense of giving up the possibility to investigate the influence of possible variations in uncertainties with the stress range level. For instance one could imagine that large stress ranges, which could potentially contribute significantly to the overall fatigue (depending on the Wöhler exponent m) may be subjected to relatively larger uncertainty than low stress ranges. Then introducing the bin-wise expected lifetimes l_j is too simplistic an approach.

It is now time to introduce the uncertainties disregarded so far, namely the model uncertainties. The common practice is to specify any model uncertainty as a random variable multiplied to the quantity that the model uncertainty relates to. This is so because the error/uncertainty typically increases with the absolute value of the quantity that the model uncertainty relates to. Though there is no general argument that the uncertainty should increase linearly with the quantity there is seldom sufficient information available to justify whether or not a linear dependency is valid, leaving the linearity assumption as the preferable choice due to its simplicity. The distribution of the model uncertainty variable is ideally of mean 1, implying no realised systematic model errors are present, i.e. no bias. The uncertainty variable's COV (Coefficient Of Variation = standard deviation / mean value) is then a convenient measure of the relative error that the model uncertainty represents. Instead of multiplicative model uncertainties one can of course consider additive errors. In practice these occur mostly in relation to measurement data, which is not really considered herein. Though one should have only a vague idea about the actual distribution of the model uncertainty variable most engineers can come up with an intuitive judgement of the relative error, which is yet another argument in favour of multiplicative uncertainties.

Take first the uncertainty of aerodynamic load modelling (see the first bulleted list in Section *Response Simulations* p. 10). These uncertainties influence the stresses. The way they influence the stresses depends on the control system of the turbine. For simplicity it is assumed, that the control system, conditional on mean wind speed, behaves approximately linearly. If X denotes some multiplicative model uncertainty to the aerodynamic load then the assumption implies that X becomes a multiplicative model uncertainty to any stress range level. Formula (2.4) shows that X^m is then the resulting model uncertainty to the sum in (2.6). In [4] four model uncertainties to the aerodynamic loads are suggested, of which only three are relevant here (the fourth is replaced by p_j)

- X_{exp} : accounts for the model uncertainties associated with the exposure, i.e. X_{exp} accounts for the uncertainties due to the modelling of terrain topography and roughness.
- X_{aero} : accounts for model uncertainties related to the assessment of the lift and drag coefficients, i.e. uncertainty originating from model-scale/full-scale disagreements and/or empirical-analytical estimates.
- X_{dyn} : accounts for model uncertainties stemming from the modelling of the dynamical response characteristics of the turbine, e.g. structural damping ratios and eigenfrequencies.

Thus the limit-state formula (2.6) is now updated to

$$g(p_j, m, \sigma', \varepsilon, X_{\text{exp}}, X_{\text{aero}}, X_{\text{dyn}}) = 1 - X_{\text{exp}}^m X_{\text{aero}}^m X_{\text{dyn}}^m \sum_j \frac{p_j l_j}{\varepsilon l_j(m, \sigma')} \quad (2.7)$$

We treat now the remaining model uncertainties. The stress analysis described in Section *Response Simulations* p. 11 involves many different model uncertainty contributions that are here gathered in just one variable X_{stress} . The uncertainty related to employing the rain flow counting algorithm instead of another stress range counting procedure is denoted X_{RFC} , and finally uncertainties re-

lated to the application of the SN-curves are put together into the variable X_{SN} . Unlike the uncertainties X_{stress} and X_{RFC} that will appear in formula (2.7) in the same way as the aerodynamic uncertainties because they are multiplied to the stress σ_i the uncertainty X_{SN} is multiplied to the number of cycles $\varepsilon^{\frac{1}{2}}(\sigma_i/\sigma')^{-m}$ meaning that X_{SN} will be divided into the other uncertainties. Thus one ends up with this final expression for the limit-state function:

$$g(p_j, m, \sigma', \varepsilon, X_{exp}, X_{aero}, X_{dyn}, X_{stress}, X_{RFC}, X_{SN}) = \\ 1 - \frac{X_{exp}^m X_{aero}^m X_{dyn}^m X_{stress}^m X_{RFC}^m}{X_{SN}} \sum_j \frac{p_j l_j}{\varepsilon l_j(m, \sigma')} \quad (2.8)$$

2.1.1 Bin-Wise Expected Lifetimes

An important part of the limit-state function is the bin-wise expected lifetimes l_j introduced in formula (2.6). These expected lifetimes have been computed for the three different materials that are used for the three different components considered in this project. Details about the computation of the bin-wise expected lifetimes, e.g. like the simplified load history shortly mentioned in Section 1.3, are given in some of the other reports of the project [5]. Here the necessary results needed in the present report are repeated and a little further developed.

For the hub and the main shaft bin-wise artificial equivalent stresses $\sigma_{e,j}$ have been determined such that they satisfy an expression of the form

$$l_j = \frac{1}{2} \left(\frac{\sigma_{e,j}}{\sigma' K_s} \right)^{-m} h \quad (2.9)$$

where 'h' denotes the time unit 'hour', and K_s is a scaling factor accounting for scale-effects and differences in surface characteristics between the test specimen and the actual component. The similarity of Equation (2.9) with the SN-curve expression $N = \frac{1}{2}(\sigma_i/\sigma')^{-m}$ is useful as it allows for scaling between different SN-curves with the same Wöhler exponent, i.e. between translated curves, without re-computing the equivalent stresses from scratch. A translation simply implies a change in σ' and no changes in equivalent stresses. It has been possible to fit a polynomial expression to the obtained $\sigma_{e,j}$ s:

$$\sigma_{e,j} = c_0 + c_1 U_{10,j}^{p_1} + c_2 U_{10,j}^{p_2} + c_3 U_{10,j}^{p_3} + c_4 U_{10,j}^{p_4} \quad (2.10)$$

The numeric values of the parameters in formulas (2.9) and (2.10) are listed in Table 1. From the employed units it is seen that the formulas give the lifetime in hours if the mean wind speed is input in m/s.

	Hub	Shaft
m	10.79	21.32
σ' [Mpa]	500	525
K_s	0.6	1.0
c_0 [Mpa]	20.19	782
p_1	1	1
c_1 [Mpa/(ms ⁻¹) ^{p₁}]	-2.76	-4.377
p_2	2	-1
c_2 [Mpa/(ms ⁻¹) ^{p₂}]	0.37	-20032
p_3	3	-1.5
c_3 [Mpa/(ms ⁻¹) ^{p₃}]	-0.00803	61623
p_4	-	-2
c_4 [Mpa/(ms ⁻¹) ^{p₄}]	-	-53270

Table 1: numeric values for the parameters in the formulas (2.9) and (2.10).

Now, the values in Table 1 are valid only for the m and σ' values specified. If the influence of uncertainties in these values is to be investigated other expressions like (2.10) are needed. As mentioned translations do not affect the expressions however changes in the exponent does. Investigations of the influence of changes in m have been made for the hub only. For a few mean wind speeds the left plot in Figure 2 depicts values of the equivalent stresses obtained with Wöhler exponents $m = m_0/\gamma$, $\gamma = 1.2, 1.1, 0.9, 0.8$ ($m_0 = 10.79$) and normalised by the fit (2.10). Changes in m are not possible without changing σ' if it is at the same time required that all of the SN-curves with changed exponent must go through a specific point. Such a requirement is enforced in the present context because the SN-curves are estimated from a set of test data. As explained in Section 2.2.2 the modelling of the statistical material data uncertainty becomes

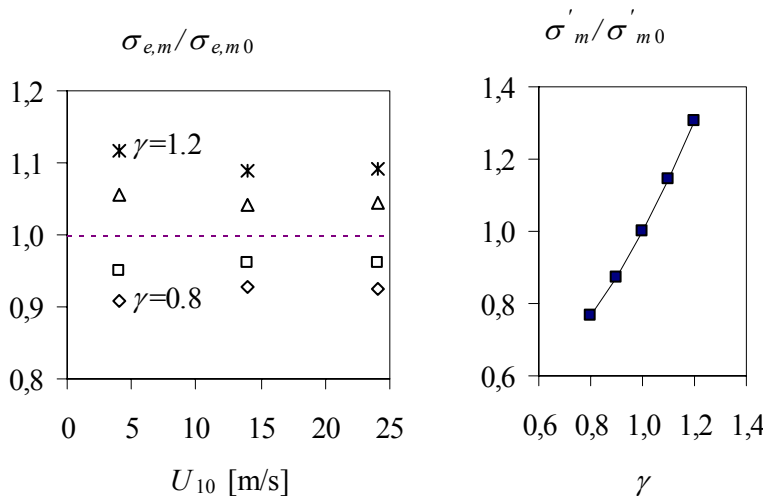


Figure 2: the influence of changes in the Wöhler exponent on the equivalent stresses (the hub material)

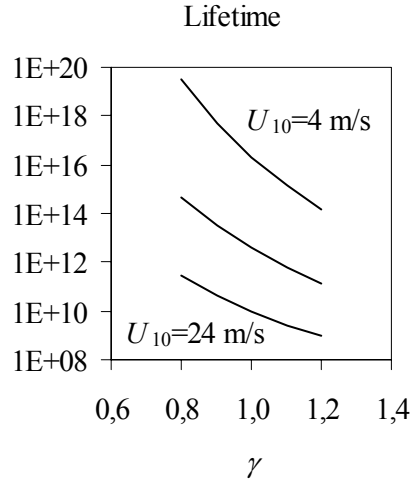


Figure 3: bin-wise expected lifetimes different Wöhler exponents of the hub material

simple if a certain average point among the test data is used as reference point. The changes in σ' following from changes in m are shown in the right plot in Figure 2. Because of the definition of equivalent stresses in this work and because of the described requirement linking m and σ' it is difficult to give intuitive arguments for the results shown in Figure 2. However Figure 3 shows that the lifetimes decrease drastically with decreasing m (increasing γ). The implication of this circumstance is discussed in Section 2.2.2. For later reference it is mentioned here that based on the data in the plots in Figure 2 the following expressions have been fitted:

$$\begin{aligned}
 \frac{\sigma_{e,m}}{\sigma_{e,m_0}} &= c_0 + c_1 U_{10} + c_2 U_{10}^2 \\
 c_0 &= 0.345\gamma^2 - 0.0915\gamma + 0.7466 \quad [(\text{m/s})^2] \\
 c_1 &= -0.0136\gamma^2 + 0.0044\gamma + 0.0091 \quad [(\text{m/s})^{-1}] \\
 c_2 &= 0.0005(\gamma - 1) \\
 \frac{\sigma'_m}{\sigma'_{m_0}} &= 0.5432 - 0.4352\gamma + 0.8917\gamma^2
 \end{aligned} \tag{2.11}$$

For the frame a simple fit like expression (2.10) has not been established. Instead interpolation between the values on the curves in Figure 4 can be made. The curve marked with the number 1.00 is obtained for the load history defined in [5]. Adding to this load history model uncertainties then, as described in Section 2.1 a scaling of the stress ranges result. If the expected lifetimes for such a scaled load history is needed one may interpolate between the curves using the numbers that mark the curves as interpolation points of the scaling factor. It is noted that unlike what is the case for the hub and main shaft, the SN-curve for the frame has been chosen among a bundle synthetic SN-curves for welded joints.

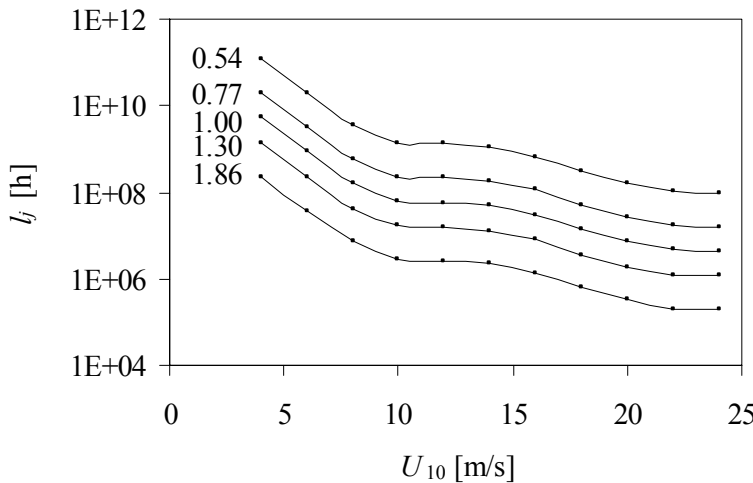


Figure 4: bin-wise expected lifetimes for the frame as function of 10-min. mean wind speed and for different ratios of the stress range to the load history ranges

2.2 Stochastic Model

2.2.1 Statistical Uncertainty of Mean Wind Distribution

The following text is based on [3]. A Weibull distribution is usually fitted to the empirical mean wind distribution:

$$F(U_{10}) = 1 - \exp\left(-\left(\frac{U_{10}}{A}\right)^k\right) \quad (2.12)$$

where A and k are distribution parameters. This distribution is assumed herein and the statistical uncertainty is expressed by stating a joint distribution of A and k . The estimation of this distribution is based on a representative synthetic Danish set of data of A s and k s estimated from one-year measurements over a

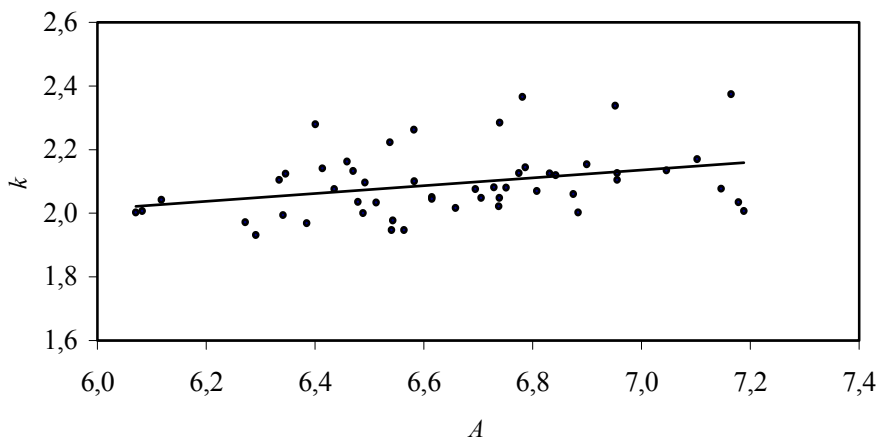


Figure 5: scatter plot of A and k

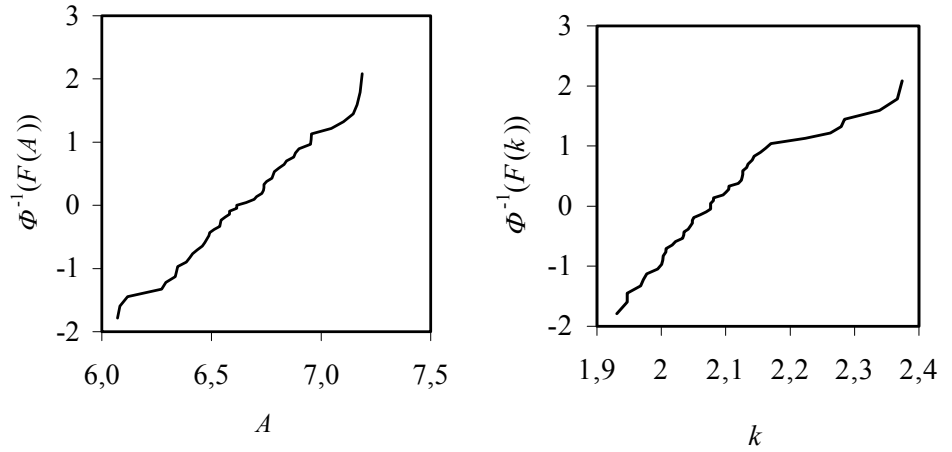


Figure 6: empirical marginal distributions of A and k .

period of 52 years. The plot in Figure 5 shows the data together with the linear regression of k on A . The parameters exhibit a weak correlation, which amounts to a correlation coefficient of 0.33.

Plotting the empirical marginal distribution functions of A and k on normal probability paper the graphs shown in Figure 6 are obtained. Assuming that A is normally distributed seems a good approximation. On the contrary the upper tail of the distribution of k is in conflict with an assumption of normality. Anticipating that the lifetime distribution is dominated by the uncertainty of the material properties it is expected that for the current purpose approximating k by a normal distribution is appropriate. This stand point is supported by the fact that COVs of A and k are 4.2% and 5.0% respectively.

An analysis of another set of data, with A and k values of the same magnitude as above but of shorter duration provide similar results. The correlation is however somewhat smaller, namely 0.22. It is therefore suggested to represent the statistical uncertainty related to the Weibull distributional parameters estimated from one-year measurements by a pair of correlated normally distributed random variables both with COV 5% and mutual correlation 0.30.

If the mean wind bins each range 2 m/s then the uncertainty of A and k enter into the limit-state function in (2.8) by substituting for p_j the expression

$$p_j = \exp\left(-\left(\frac{U_{10,j} - 1}{A}\right)^k\right) - \exp\left(-\left(\frac{U_{10,j} + 1}{A}\right)^k\right) \quad (2.13)$$

where $U_{10,j}$ equal the bin centres, and (A, k) follows the suggested joint probability distribution.

2.2.2 Inherent and Statistical Uncertainty of Material Data

In this section the focus is put on the uncertainties attached to SN-curves derived from data. The uncertainties related to the application of synthetic curves are not discussed, as the subject is not part of the project plan. We will consider the data plotted in Figure 7. That data, which is taken from [5], corresponds to

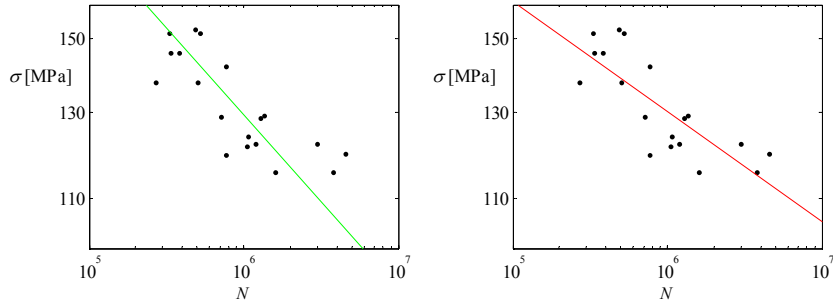


Figure 7: test data from representative cast steel material used for hubs. Left plot is correct.

the hub, and will be extensively used in the following as a reference case. Before proceeding to the derivation of the stochastic model for the uncertainties, a discussion of how to properly obtain by statistical means the SN-curve from a set of test data is given.

Because fatigue tests are designed the way they are, i.e. a constant stress amplitude is fixed and then the experiment is run – preferably – until rupture, the only statistical sound estimation approach is to estimate the linear regression of $\log N$ (the dependent variable) on $\log \sigma$ (the independent variable). The argument is as follows. The core of any regression analysis is a stochastic model. In the simplest case, which is considered here, the stochastic model assumes that the dependent variable is random with a mean value that depends on the independent variable, which is deterministic. Since the only way to conduct fatigue tests is to choose the stress amplitude deterministically and obtain the lifetime as a random result, it is evident that the proper regression analysis is to estimate $\log N$ as the linear regression on $\log \sigma$. Trying the opposite is algebraically possible, though meaningless, and it will generally lead to too large a Wöhler exponent m , the overestimation being lesser the lesser the data spreads about the regression line. That is, a non-conservative estimate of lifetimes for stresses below the average stress range of the tests, and a conservative estimate for stresses above the average, follows. The reason for the over-estimation of the Wöhler exponent lays in the fact that in the estimator of the slope of the regression line those points that – measured along the axis of the variable chosen as the independent variable – lay furthest away from the centre of gravity of the data get the highest weights. Figure 7, Figure 8 and Figure 9 illustrate the differences between the correct and the wrong approach. In Figure 7 both the lim-

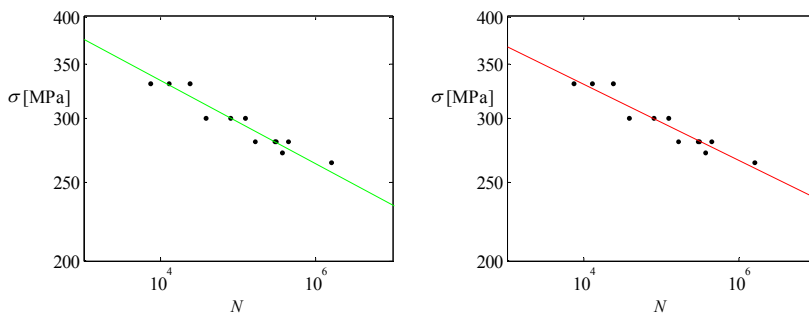


Figure 8: test data from representative high-strength steel used for shafts. Left plot is correct.

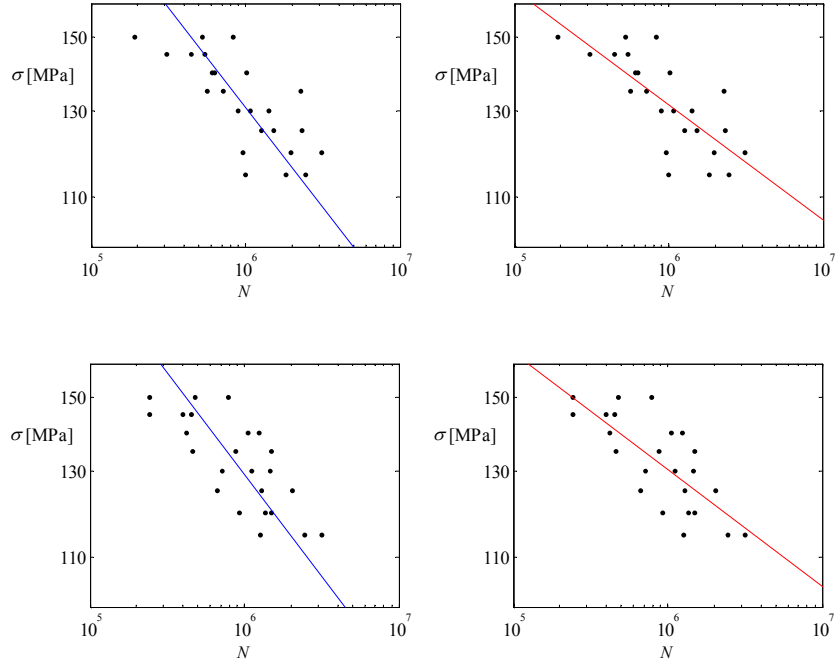


Figure 9: artificially simulated test data for visual judgement of goodness of slope estimates. Left plots are correct.

ear regression of $\log N$ with respect to $\log \sigma$ and vice versa appear; left-hand plot and right-hand plot respectively. The correct and the wrong estimates are in this case considerably different, $m = 6.83$ and $m = 10.79$ respectively. Figure 9, which has been obtained artificially by numerical simulation, shows more clearly than Figure 7 that the wrong estimate tends to cut through the data along the diagonal rather than along the centre line of the data giving in that way an optimistic estimate of the Wöhler exponent. If the spread in data is less than shown in Figure 7 and Figure 9 then the differences between the two ways of determining the linear regression becomes less. Figure 8, showing the two regression lines for the set of high-strength steel data used for the shaft in this work, is such an example where one obtains $m = 19.6$ and $m = 21.3$ for the correct and wrong slope, respectively.

It is now time to turn to the quantification of the statistical and inherent uncertainty of the material strength. It is convenient to parameterise the linear regression model as

$$\log N = \alpha + \beta(\log \sigma - \overline{\log \sigma}) + \log \varepsilon \quad (2.14)$$

where $\overline{\log \sigma}$ denotes the sample average of the logarithmised stress ranges in the data set. The parameterisation exploits that the linear regression goes through the point of gravity of the logarithmised data set. The m and σ' relate to the α , β , and $\overline{\log \sigma}$ through

$$\begin{aligned} m &= -\beta \\ \sigma' &= e^{\overline{\log \sigma}} (2e^\alpha)^{-1/\beta} \end{aligned} \quad (2.15)$$

The ε in (2.14) is identical to the ε in $N_i = \varepsilon^{\frac{1}{2}}(\sigma_i/\sigma')^{-m}$. Substituting (2.15) into $N_i = \varepsilon^{\frac{1}{2}}(\sigma_i/\sigma')^{-m}$ yields the expression that will form the basis of the inclusion of the statistical and inherent uncertainties of the material strength:

$$N = \left(\frac{\sigma}{e^{\log \sigma}} \right)^\beta e^\alpha \varepsilon \quad (2.16)$$

The inclusion of the uncertainties is obtained by substituting the α and β by their estimators $\hat{\alpha}$ and $\hat{\beta}$ which are random variables. Under the usual assumption that the inherent randomness covered by the residuals $\log \varepsilon$ be zero mean normal distributed the estimators follow a normal distribution with parameters that can be estimated from the data. Also the std. dev. s of the residuals is substituted by its estimator \hat{s} , which is qui-square distributed. Denoting by s and k the estimated std. dev. of the residuals and the number of data points, respectively, then

$$\begin{aligned} \hat{\alpha} &\in N(\overline{\log N}, \frac{s^2}{k}) \\ \hat{\beta} &\in N(\frac{S_{\log \sigma \log N}}{S_{\log \sigma \log \sigma}}, \frac{s^2}{S_{\log \sigma \log \sigma}}) \\ \log \varepsilon &\in N(0, \hat{s}^2), \quad \hat{s}^2 \in \frac{s^2}{k} \chi^2(k-2) \end{aligned} \quad (2.17)$$

where

$$\begin{aligned} s^2 &= \frac{S_{\log N \log N} - S_{\log \sigma \log N}^2 / S_{\log \sigma \log \sigma}}{k-2} \\ S_{\log \sigma \log \sigma} &= \sum_{l=1}^k (\log \sigma_l - \overline{\log \sigma})^2 \\ S_{\log N \log N} &= \sum_{l=1}^k (\log N_l - \overline{\log N})^2 \\ S_{\log \sigma \log N} &= \sum_{l=1}^k (\log \sigma_l - \overline{\log \sigma})(\log N_l - \overline{\log N}) \end{aligned} \quad (2.18)$$

It is noted that the applied modelling of the statistical uncertainty follows from Bayesian statistics assuming standard non-informative prior distributions. Different choices could have been made, however, this is not discussed in any further detail here. The estimated numeric values of the parameters in (2.17) for the hub material are stated in Table 2. Clearly the translation parameter α is well determined, whereas the slope parameter β has a COV a little below 20%. Also the inherent randomness contributes a considerable amount. Figure 10 that shows three different 95 percent confidence intervals supports these observa-

k	$\overline{\log N}$	$\overline{\log \sigma}$	s	$S_{\log \sigma \log \sigma}$	$S_{\log \sigma \log N}$	$S_{\log N \log N}$
19	13.7	4.88	0.513	0.164	-1.12	12.12

Table 2: estimated distributional parameters of the statistical uncertainty model for the hub material strength.

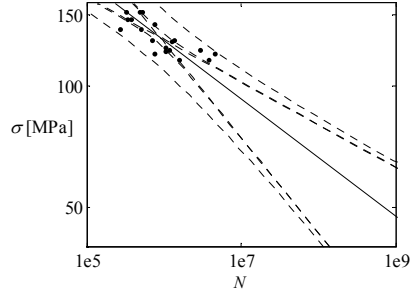


Figure 10: 95% confidence intervals for the regression line and for the regression model. See the text for further details.

tions. The innermost interval is the confidence interval for the regression line when neglecting the uncertainty of the translation term. The middle curve is the confidence interval for the regression line when including the uncertainty of the translation term. It is seen that the uncertainty of the translation term does not contribute much outside the core of the data set. The outermost curve is the confidence interval of the regression model, i.e. the regression line plus the residuals (the uncertainty of the estimation of s^2 has been disregarded). Clearly the inherent randomness contributes much, even as one moves away from the centre of the data set.

In the present report the inherent uncertainty of the material strength is described as the uncertainty of the number of cycles to rupture. When looking into e.g. design standards the inherent uncertainty is often described as an uncertainty of the stress range. This is not in conflict with the presentation here because having first estimated the parameters of the regression model in the correct way explained earlier in this section nothing prohibits rearranging Equation (2.14) into

$$\log \sigma = \frac{\log N - \alpha}{\beta} + \overline{\log \sigma} - \frac{\log \varepsilon}{\beta} \quad (2.19)$$

in which the inherent uncertainty now appears as an uncertainty to the stress ranges. A scaling of the std. dev. accounting for the slope has of course taken place but the confidence intervals are the same for the formulations (2.14) and (2.19) as they are fully equivalent.

The std. dev. estimate $s = 0.513$ stated in Table 2 corresponds to the test data covering about $\frac{3}{4}$ of a decade around the regression line. Since this is just one single estimate gathering other information is of interest. Asking an expert [7], he says that for materials with Wöhler exponents about 3 the test data covers approximately $\frac{1}{2}$ of a decade about the regression line at all stress range levels. This appears to be in good agreement with the estimate. In Section 2.3 results for different values of s are presented.

Formula (2.16) gives an expression for the number of cycles to rupture in terms of the parameters α and β . What is needed for the limit-state function (2.8) is an expression for the bin-wise expected lifetimes in terms of the estimators for the parameters α , β and s . Because of the similarity between the SN-curve expression and the formula (2.9) one easily derives that

$$l_j = \left(\frac{\sigma_{e,j}(\hat{\beta})}{e^{\log \sigma} K_s} \right)^{\hat{\beta}} e^{\hat{\alpha}} \varepsilon \text{ h} \quad (2.20)$$

where $\hat{\alpha}$, $\hat{\beta}$ and \hat{s} are the estimators defined by formulas (2.17).

Because the mean value of $\hat{\beta}$ for the hub material is numerically notably smaller than the wrong estimate used as reference for the calculations recapitulated in Section 2.1.1 the formulas (2.11) will be used for extrapolation far from the data that the formulas are fitted to. However, as the results depicted in Figure 3 show substantial reductions in the lifetime of the hub with lower Wöhler exponents, it is worth investigating the consequences of using the correctly estimated slope rather than the wrong slope, even though this study will be uncertain in itself. The fact that the bin-wise lifetimes decrease with the slope reflects that the fatigue stress ranges acting on the hub material are below the average test stress range. It is exactly in such a case the sensitivity of the lifetime distribution to the uncertainty of the correct estimate of the Wöhler exponent is most relevant.

2.2.3 Model Uncertainties

As mentioned earlier substantiating choices of model uncertainty distributions is difficult. Since the distribution of the model uncertainties is usually unknown choosing a symmetric distribution is a reasonable choice. Due to its simplicity the Gaussian distribution is often the favourite among the symmetric distributions. For small COVs (up to at most 10%) the Gaussian and the Log-Normal distributions do not deviate much from each other. Because the product of Log-Normal distributions is again a Log-Normal distribution choosing this as the model uncertainty distribution is convenient. Therefore the Log-Normal distribution is in this context preferred to the Gaussian. Thus in the remainder of this report all the model uncertainties are simply replaced by one variable

$$X = \frac{X_{\text{exp}}^m X_{\text{aero}}^m X_{\text{dyn}}^m X_{\text{stress}}^m X_{\text{RFC}}^m}{X_{\text{SN}}} \quad (2.21)$$

If one denotes by a V the coefficient of variation one can show that

$$1 + V^2 = \left[(1 + V_{\text{exp}}^2)(1 + V_{\text{aero}}^2)(1 + V_{\text{dyn}}^2)(1 + V_{\text{stress}}^2)(1 + V_{\text{RFC}}^2) \right]^{m^2} (1 + V_{\text{SN}}^2) \quad (2.22)$$

Obviously those model uncertainties that are multiplied directly to the stress are considerably magnified according to the slope of the SN-curve. The mean value of the X is, if one assumes that of all the X 's have mean value 1,

$$E[X] = 1 + V_{\text{SN}}^2 \quad (2.23)$$

Having now at hand the expressions (2.22) and (2.23) the question regarding the values of the COVs emerge. The work in [4] suggests some values for V_{exp} , V_{aero} , and V_{dyn} based on further references given in [4] – namely 10%, 10% and 5% respectively. In Section 3.2 alternative values of the COVs of the model

COV	V_{exp}	V_{aero}	V_{dyn}	V_{stress}	V_{RFC}	V_{SN}
Value	0.10	0.10	0.05	0.05	0.02	0.05

Table 3: example of model uncertainty quantification

uncertainties are further discussed. The other model uncertainties are believed to be in the same range. Whether this postulate is true or not is not discussed any further but instead the results of computations with different model uncertainties are shown in Section 2.3. An example of the choice of the model uncertainties could be as stated in Table 3. This example leads to the following total model uncertainty COV if $m=1, 3$ and 10 , respectively: $0.17, 0.51$ and 3.40 . These numbers show the influence of the slope. The first case is not realistic, but has been included for reference as it corresponds to no magnification of uncertainties. The second corresponds to structural steel, whereas the third is for cast steel. In the latter case COV of the total uncertainty is no longer small. Because the upper tail of the Log-Normal distribution is thick compared to that of the Gaussian distribution the seemingly harmless choice of using the Log-Normal distribution for the individual uncertainties instead of the Gaussian does have quite an impact on the total uncertainty distribution. Whether to choose other distribution types is not discussed any further.

2.3 Results

In this section the lifetime distributions $F(l)$ for different situations are shown. In order to facilitate the future use of the results presented here various sensitivity studies are carried out. All plots show a limited part of the lower tail of $F(l)$ because the components are of course designed to have low probabilities of failure. Since wind turbines are generally designed with the requirement that the time of operation should be 20 years the lower tail from 20 years to 500 years is considered. The plots are made on normal probability paper with probabilities ($p_f(l) = F(l)$) on the left-hand ordinate-axis and the corresponding reliability indices on the right-hand ordinate axis. The reliability index β is defined by $\beta = -\Phi^{-1}(p_f)$ where $\Phi^{-1}(\cdot)$ designates the inverse of the standard Gaussian distribution. For all computations the average 10-min. mean wind speed has been set to $V_{\text{ave}} = 8.5$ m/s.

We start out by considering the hub component as it allows for the widest spectrum of sensitivity studies. Because the model uncertainties are of identical type the sensitivities of the lifetime distribution with respect to V_{exp} , V_{aero} , V_{dyn} , V_{stress} and V_{RFC} are similar. The sensitivity with respect to V_{SN} will be different from these sensitivities because X_{SN} appears in a different place in the limit-state function (2.8). Figure 11 shows the sensitivity with respect to V_{stress} and V_{SN} in the case where the statistical uncertainty, originating from the limited number of test data, of the SN-curve is neglected. The other model uncertainties are set as stated in Table 3. The Wöhler exponent and the standard deviation of the spread ε of the lifetimes around the SN-curve are taken from Table 2. Owing to the fact that X_{stress} is raised to the power of the Wöhler exponent the sen-

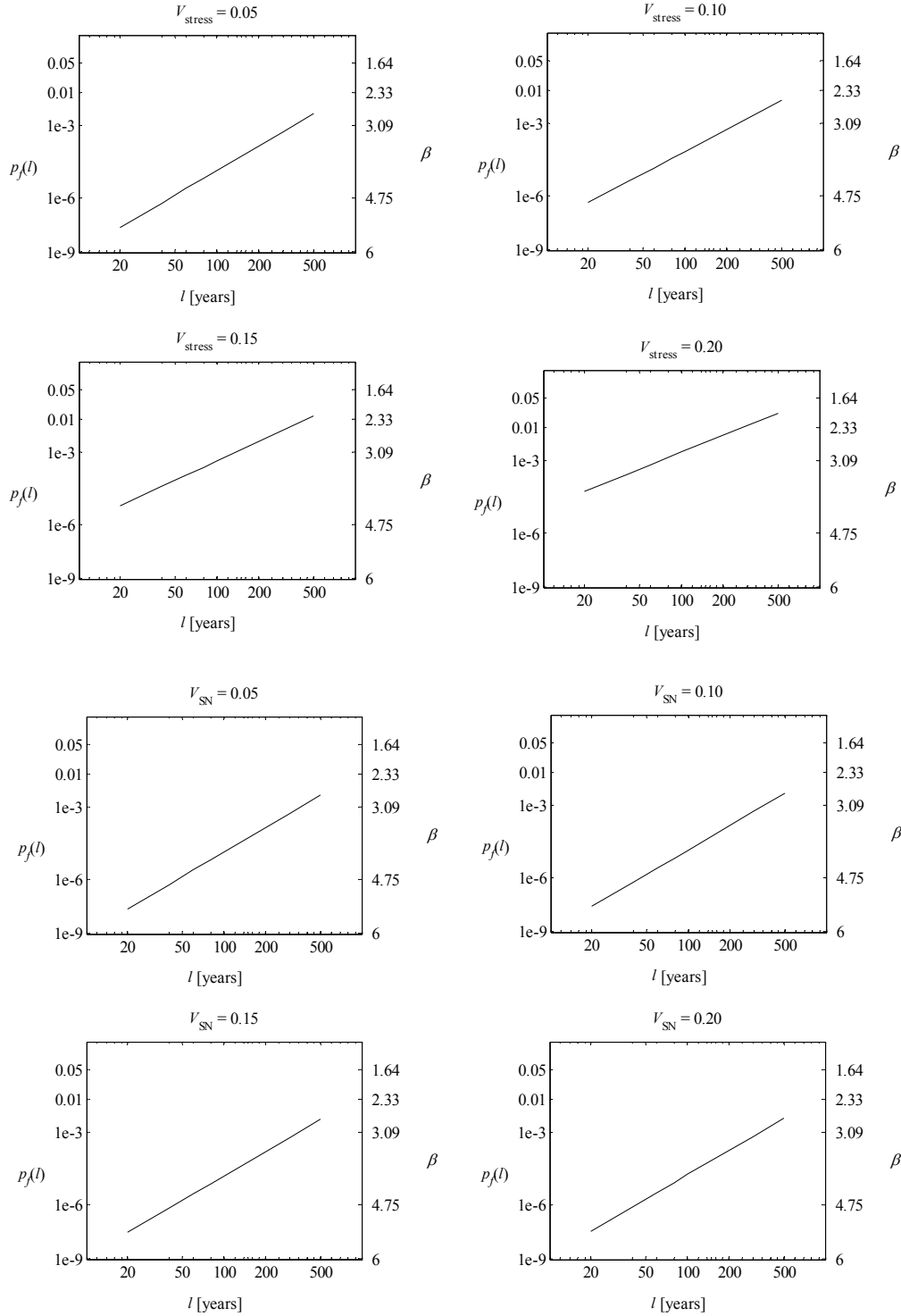


Figure 11: sensitivity of lifetime distribution for the hub with respect to COV of model uncertainty X_{stress} and X_{SN} respectively. No statistical uncertainty of the SN-curve.

sensitivity with respect to V_{stress} is considerably larger than the sensitivity with respect to V_{SN} that is practically non-existing.

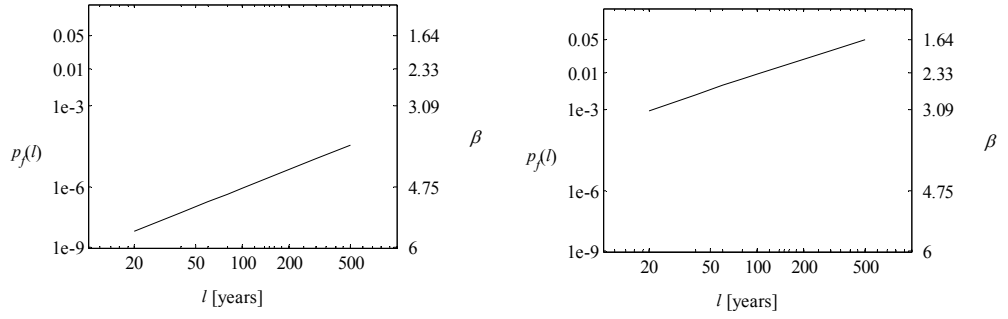


Figure 12: left-hand plot shows the lifetime distribution of the hub with a wrong Wöhler exponent (no statistical uncertainty of the SN-curve). The right-hand plot is the lifetime distribution with correct Wöhler exponent and statistical uncertainty of the SN-curve. In both cases model uncertainties are taken from Table 3.

The plots in Figure 12 illustrate the importance of modelling the SN-curve correctly. The left-hand plot in Figure 12 shows, still in the case of neglecting the statistical uncertainty of the SN-curve, the influence of applying the wrong, i.e. the too optimistic, Wöhler exponent. Comparing the plot to the uppermost left-hand plot in Figure 11 it shows that for the present case the safety is increased approximately by an order of magnitude. The right-hand plot in Figure 12 shows the impact of the statistical uncertainty of SN-curve on the lifetime distribution. Though a wrong Wöhler exponent can result in underestimated lifetime distributions the present case shows that the statistical uncertainty has much more importance. The plots in Figure 11 showed that the sensitivity with respect to V_{stress} is notable when the ideal situation of no statistical uncertainty

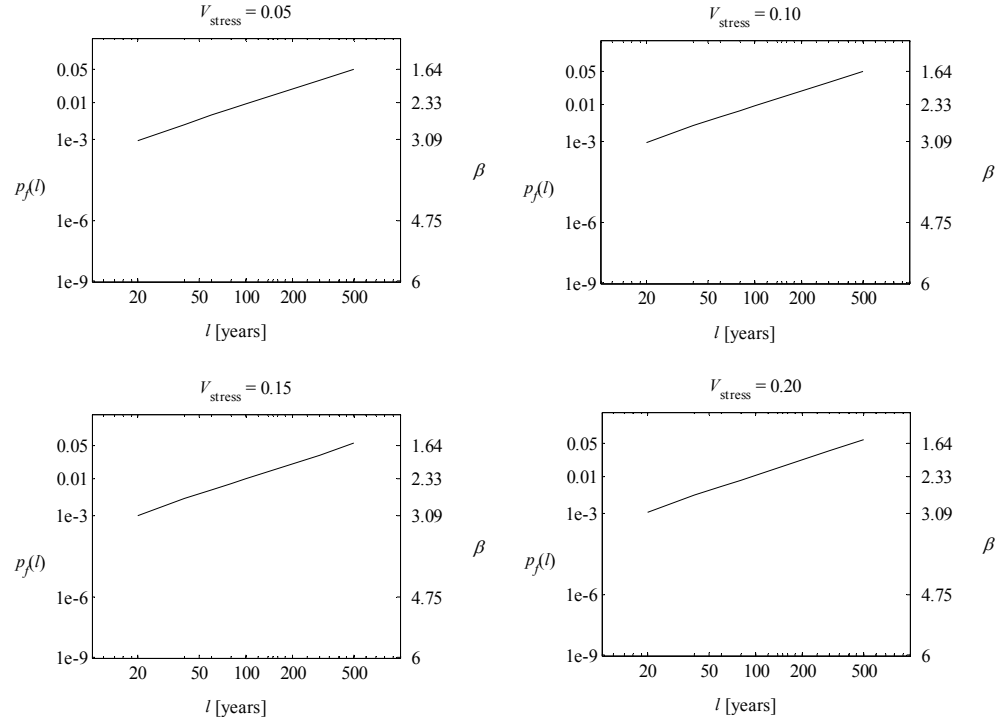


Figure 13: sensitivity of lifetime distribution of the hub with respect to COV of model uncertainty X_{stress} in case of statistical uncertainty of the SN-curve.

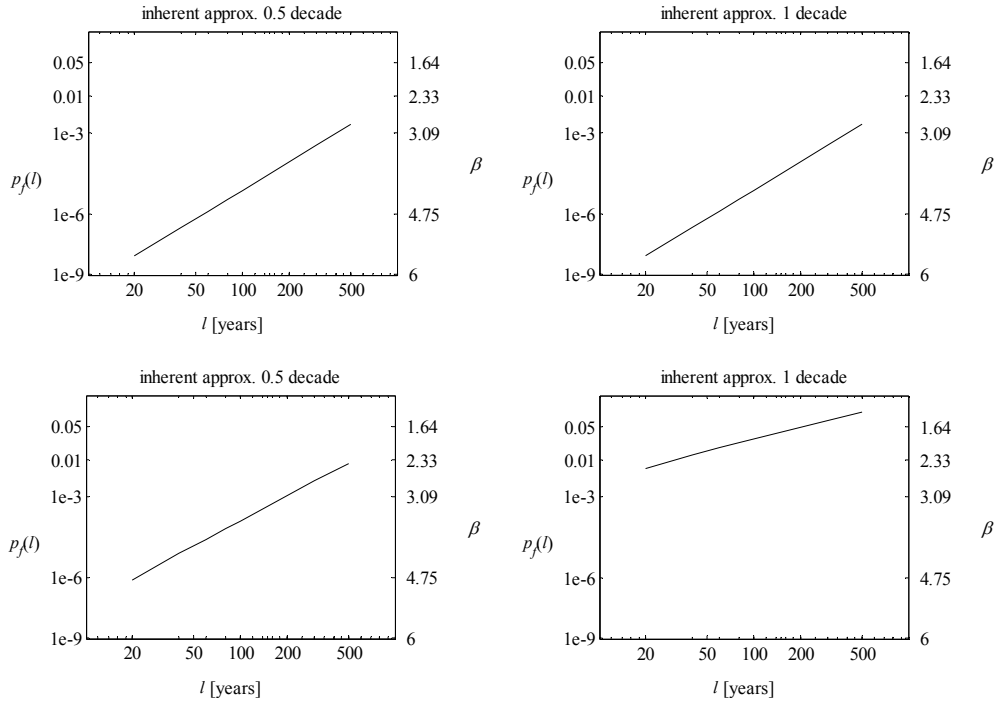


Figure 14: sensitivity to inherent randomness of lifetime distribution of the hub; first row does not include statistical uncertainty of SN-curve; the second row does. Model uncertainties are taken from Table 3.

of the SN-curve is considered. On the other hand Figure 13 shows that when the statistical uncertainty of the SN-curve is included the sensitivity to V_{stress} practically vanish.

Because the COV of the spread ε of the lifetimes around the SN-curve is not always easy to assess it is also of interest to see what is the sensitivity to this parameter – i.e. the sensitivity to the inherent material randomness. The COV is characterised by the fraction of a decade on the lifetime axis that is covered by 4 times the standard deviation of $\log \varepsilon$. The first row of plots in Figure 14 shows the sensitivity in case the statistical uncertainty of the SN-curve is neglected. The lifetime distribution is not much sensitive to the COV of the inherent material randomness because, like it is the case with the model uncertainty V_{SN} , ε is

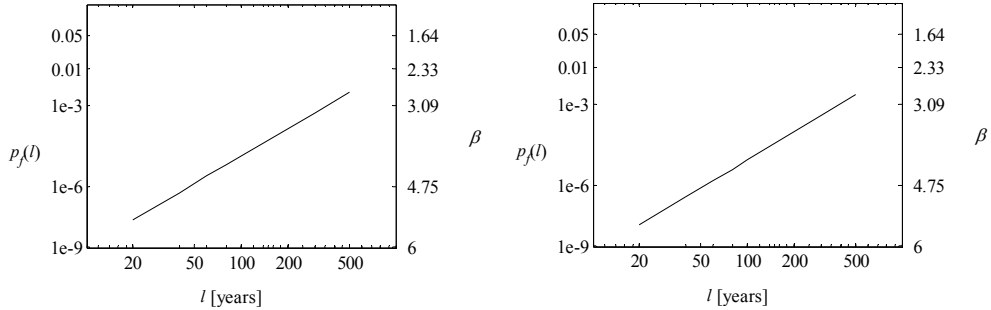


Figure 15: sensitivity of the lifetime distribution of the hub to statistical uncertainty of the mean wind distribution. In the left plot the uncertainty is neglected. Model uncertainties are taken from Table 3.

not amplified by the Wöhler exponent. Contrary to this the second row of plots in Figure 14 shows the sensitivity in case the statistical uncertainty of the SN-curve is not neglected. In that case, the sensitivity becomes large because the statistical uncertainty of the SN-curve scales with the COV of ε – see Formulas (2.17).

Finally, in Figure 15 the sensitivity of the lifetime distribution with respect to the statistical uncertainty of the mean wind distribution is illustrated in the case of no statistical uncertainty of the SN-curve. Comparing the left-hand plot in which the statistical uncertainty has been disregarded to the right-hand plot in which the statistical uncertainty of the mean wind distribution is included shows that the sensitivity is very small. It is noted that the statistical uncertainty of the mean wind distribution as described in 2.2.1 considers that the mean wind distribution is estimated from one year of measurements. Basing the mean wind distribution estimate on more than one year will bring the sensitivity further down. Moreover, if statistical uncertainty of the SN-curve is introduced the sensitivity to the statistical uncertainty of the mean wind distribution becomes even smaller.

We now turn to the main shaft for which the SN-curve is also based on test data. Since a detailed analysis of sensitivities to statistical uncertainty of SN-curves was given in relation to the hub component such analysis is not conducted for the main shaft. Only a few results are given. Figure 16 shows the sensitivity with respect to V_{stress} in the case where the statistical uncertainty of the SN-curve is neglected. The other model uncertainties are set as stated in Table 3. The Wöhler exponent and the standard deviation of the spread ε of the lifetimes around the SN-curve are computed from the test data and they are

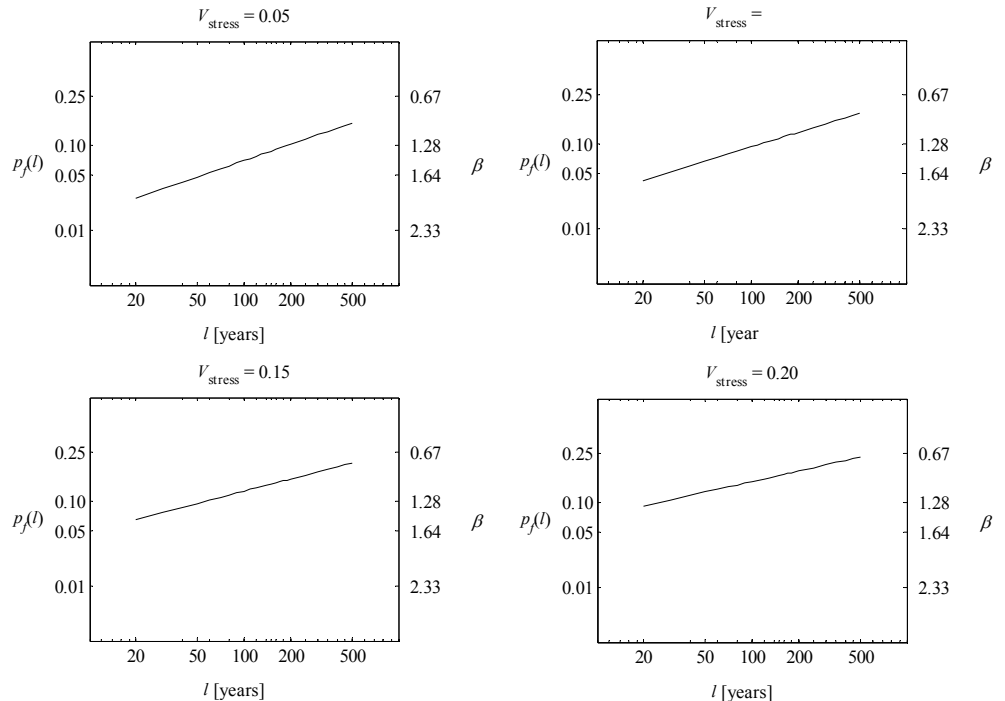


Figure 16: sensitivity of lifetime distribution for the main shaft with respect to COV of model uncertainty X_{stress} . No statistical uncertainty of the SN-curve.

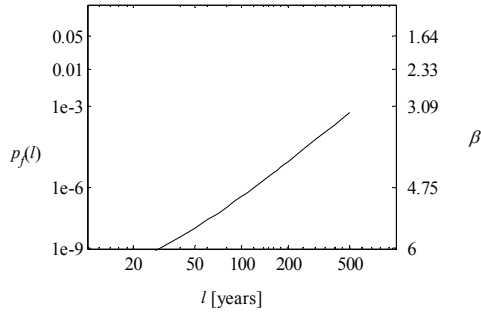


Figure 17: the lifetime distribution for the frame with model uncertainties taken from Table 3 except V_{SN} has been set to 0.15.

$m = 21.32$ and $\hat{s} = 0.48$. Again it is seen that, as it was the case for the hub, that the lifetime distribution is sensitive to V_{stress} . More interesting it is to see that the probability of failure for 20 years is in the order of 5% to 10% for the shaft – even when not accounting for statistical uncertainties of the SN-curve – which is considerably higher than for the hub that has a probability of failure of 1% when also including statistical uncertainty of the SN-curve. This is further discussed below.

Contrary to the main shaft the frame is safer than the hub component – this appears from Figure 17 that shows the lifetime distribution of the frame. This distribution is based on a synthetic SN-curve implying that no explicit statistical uncertainty of the SN-curve exists. To counter for this the COV V_{SN} of the model uncertainty X_{SN} has been set to 0.15, otherwise the model uncertainties from Table 3 has been used. Bearing in mind the lesson learned from the hub component, that statistical uncertainty of the SN-curve dominates the lifetime distribution and that the sensitivity to V_{SN} is small one could argue that setting V_{SN} to 0.15 does not really counter the statistical uncertainty that must be present in the data that has once lead to the synthetic SN-curve. However one must anticipate that more test data is behind the synthetic SN-curves than the specific ones considered here implying less sensitivity to the statistical uncertainty of the SN-curve. The Wöhler exponent is 3 and the COV of the inherent randomness of the lifetimes has been set so that 4 times the standard deviation of $\log \varepsilon$ corresponds to $\frac{1}{2}$ a decade on the lifetime axis. This choice is based on [7].

The question is now what can be the reasons that the three components have so different levels of safety. It is first noted this can be explained by the fact that three different manufacturers have contributed each with one of the components to the generic turbine considered in this work. The differences are therefore expected to result partly from the fact that different manufacturers may have different design strategies, partly from the fact that in any turbine not all components are designed fully to the limit. Thus any turbine design has a bottleneck, which then can be one of the components considered herein, i.e. the main shaft. It is noted, however, that the safety of the shaft seems to be very low, implying that other reasons than the bottleneck-argument may exist. These have not been uncovered during the course of the project. The reason that the frame has very high reliability can be that the design strategy applied implies very conservative assessment of characteristic loads and design loads.

3 Reliability Considerations

Equation Chapter (Next) Section 1 In this chapter some preliminary investigations of how partial safety factors for fatigue can be adjusted if one can reduce model uncertainties are given. The investigations do not include inspection planning, which can excessively reduce safety factors. The way the stress range counting has been performed in the current project puts some limitations on the general validity of the results, and only the hub component is considered.

3.1 The Calibration Procedure

The procedure employed here to compute the effects on the partial safety factors of changes in the uncertainties is called calibration. The kind of calibration regarded here is the one where existing safety factors and related characteristic values corresponding to a specific uncertainty model are given and another set of partial safety factors for the same characteristic values and a modified yet comparable uncertainty model is sought. By an uncertainty model is meant a listing of uncertainty sources and their quantification – just like presented in the previous chapter. The aim is that the level of reliability of components designed according to the derived safety factors and subject to the modified uncertainty model must be equal to the reliability level of components designed according to the existing safety factors and subject to the corresponding uncertainty model. The reliability level of the components designed according to the existing safety factors is therefore termed the target probability and the calibration technique could be called ‘probabilistic calibration’. The technique consists in the following 4 steps:

1. Design a component using the existing safety factors and characteristic values. The design must be ‘to the limit’.
2. Compute the reliability of the designed component according to a specific uncertainty model believed to correspond to the safety factors. This reliability is then the target reliability level.
3. Design a component that, according to the modified uncertainty model, will have reliability equal to the target. This design will have other dimensions than the component obtained in step 1.
4. Determine the safety factors that, applied to the characteristic values, will result in loads and material strengths that will lead to a design equal to that obtained in step 3.

In steps 1 and 4 the so-called design equation is employed. The design equation has many similarities to the equation that defines the zero-points of the limit-state function. The design equation is defined by (see Eq. (2.3)):

$$\sum_j p_{c,j} l \sum_i \frac{n_{c,ij}}{\varepsilon^{\frac{1}{2}} (\gamma_f \sigma_{c,i} / (\sigma'_c / \gamma_m))^{-m_c}} = 1 \quad (3.1)$$

All model uncertainty variables are removed and the load and strength variables are replaced by characteristic values (indicated by an index ‘c’) and partial

safety factors γ_f and γ_m for load and material respectively. The stress ranges $\sigma_{c,i}$ stems from internal cross-sectional loads $Q_{c,i}$ that are scaled by some influence number, say z , reflecting the design of the component. It is the value of z – in the following termed the design parameter – that is determined in steps 1 and 3. Introducing the design parameter in the design equation (3.1) one gets

$$\sum_j p_{c,j} l FDF \sum_i \frac{n_{c,ij}}{\frac{1}{2}(z Q_{c,i} / \sigma'_c)^{-m_c}} = 1 \quad (3.2)$$

In which also $FDF = (\gamma_m \gamma_f)^{m_c}$, the often-used so-called Fatigue Design Factor, has been introduced as a factor to the lifetime.

Because in this project the manufacturers have provided the design of the components and because, for confidentiality reasons, they have not supplied all details on the design procedure the partial safety factors to be used in step 1 are not known. This means the fatigue design factor has to be derived herein. This is done on the assumptions that:

- a. the components have been designed to the limit,
- b. that the load safety factor has been put to 1.0, and
- c. that the characteristic value of the number of cycles to fatigue (or similar the material fatigue strength) is determined by the mean value minus two times the standard deviation of the natural randomness of the lifetime (or fatigue strength).

Assumption ‘a’ implies that the design parameter z to be assessed in step 1 has already been determined by the manufacturer. From the assumption ‘b’ it follows that the loads applied in the calculations, which have led to the bin-wise expected lifetimes presented in Section 2.1.1, are the characteristic loads. Combining this with assumption ‘c’ it implies the characteristic expected lifetimes $l_{j,c}$

equals the computed expected lifetimes multiplied by e^{-2s} , where s denotes the standard deviation of the logarithm of the natural randomness, ε , of the lifetimes (see Equation (2.17)). The calibration procedure requires the possibility to compute the bin-wise expected lifetimes for different designs, that is for different values of the design parameter z . Assuming further that the stresses scale linearly with z and introducing the ratio $\eta = z_0/z$, where z_0 denotes the reference design parameter corresponding to the design provided by the manufacturer, the design equation can finally be restated as:

$$\sum_j \frac{p_{c,j} l FDF}{\eta^{m_c} e^{-2s} l_j(m_c)} = 1 \quad (3.3)$$

where $l_j(m_c)$ denotes the bin-wise expected lifetimes obtained with the characteristic value of the Wöhler exponent defined here as the expected value, i.e. for the hub material $m_c = 6.83$. The limit-state function corresponding to the derived design equation is (see Equation (2.8))

$$g(p_j, m, \sigma', \varepsilon, X_{\text{exp}}, X_{\text{aero}}, X_{\text{dyn}}, X_{\text{stress}}, X_{\text{RFC}}, X_{\text{SN}}) = 1 - \frac{X_{\text{exp}}^m X_{\text{aero}}^m X_{\text{dyn}}^m X_{\text{stress}}^m X_{\text{RFC}}^m}{X_{\text{SN}}} \sum_j \frac{p_j l}{\varepsilon l_j(m, \sigma') \eta^{m_c}} \quad (3.4)$$

Based on Equations (3.3) and (3.4) the four steps of the calibration procedure may be implemented for the current problem by the following four steps (note that, in accordance with the above made assumptions step 1 is replaced by a determination of the current safety factors):

1. Assuming that the component is designed to the limit put $\eta = 1$, $l = 20$ years, and solve the design Equation (3.3) with respect to FDF , giving the partial safety factor product $\gamma_m \gamma_f = \sqrt[m]{FDF}$.
2. For $l = 20$ years and $\eta = 1$ use the limit-state function (3.4) to assess the target reliability level denoted β_t .
3. With the modified uncertainty model use the limit-state function (3.4) to determine η such that for $l = 20$ years the reliability β_t is obtained.
4. With the η obtained in step 3 and $l = 20$ years solve again the design equation (3.3) with respect to FDF , giving the new calibrated partial safety factor product $\gamma_m \gamma_f = \sqrt[m]{FDF}$.

Before proceeding to the results a remark on the assumed definition of the characteristic SN-curve is appropriate. The assumed definition corresponds to a parallel shift of the SN-curve sideways to the left giving an SN-curve corresponding approximately to the 2.3 percentile. Other definitions could be relevant. For other definitions other FDF 's will come out of step 1 in the above procedure. Knowing the ratio between the characteristic SN-curve assumed here and any other characteristic SN-curve, the partial safety factor product $\gamma_m \gamma_f$ can be directly scaled by this ratio.

3.2 Results

In this section only results for the hub material are shown. The uncertainty model developed in Chapter 2 is of course used here as starting point. The values suggested in Table 3 are – as mentioned – based on [4]. In [4] other possible values than the ones adopted in Table 3 are given. In [4] it is argued that putting $V_{\text{exp}} = 10\%$, $V_{\text{aero}} = 10\%$, and $V_{\text{dyn}} = 5\%$ is the minimum uncertainties that can be reasonably obtained. Typically the computer models of any wind turbine are calibrated to fit with full-scale response measurements. Naturally the uncertainties of the computer model cannot be smaller than the uncertainties of the measurements, which in [4] is judged to be 10% for the aerodynamic loads and 5% for the dynamical properties such as eigenfrequencies and damping ratios. In other works than [4] it is suggested to put $V_{\text{exp}} = 20\%$. In [4] the argument is that by use of programs like WASP or by site measurements of the climate the effects of the terrain (topography) can be accurately accounted for why V_{exp} can be put equal 10%. So, essentially the values suggested in Table 3 are – in the author's opinion – the least conservative uncertainty model that can be used. Because the author also finds the values fairly realistic they have been used for the study of the lifetime distributions. In the present section two cases are considered: 1) a case where the values in Table 3 are assumed realistic, and the consequences for the partial safety factors of having even lower model uncertainties is examined, and 2) a case where higher model uncertainties are assumed as reference uncertainties and the consequences for the partial safety factors of having the model uncertainties reduced to the ones suggested in Table 3.

$\beta_t = 5.43$	V_{exp}	V_{aero}	V_{dyn}	V_{stress}	V_{RFC}	V_{SN}	η	FDF	$\gamma_m \gamma_f$
Reference	0.10	0.10	0.05	0.05	0.02	0.05	1	873	2.69
Exposure	0.05	-	-	-	-	-	.89	394	2.40
Aerodyn.	-	0.05	-	-	-	-	do.	do.	do.
Dynamics	-	-	0.03	-	-	-	.975	734	2.63
Exp.+aero	0.05	0.05	-	-	-	-	.775	153	2.09
All three	0.05	0.05	0.03	-	-	-	.751	124	2.02

Table 4: calibrated partial safety factor products for the hub material when statistical uncertainty of the SN-curve is disregarded. The first row gives the reference model uncertainties as stated in Table 3. In the second to the sixth row a dash means that the reference value given in the first row is used. β_t is given in the upper left corner.

The first case is included to provide guidance for those that can document that they can actually obtain lower uncertainties than the author considers to be minimum. The latter case is motivated by the fact that the partial safety factors currently stated in wind turbine standards have originally been developed for building codes from where they have been adopted. One could therefore argue that they correspond to higher model uncertainties than suggest in Table 3 why the partial safety factors should be calibrated to become lower, so that they correspond to the present day practise of wind turbine engineering. Because this is a point of view that can be discussed the current work gives only the results of these various assumptions without suggesting possible adjustments of partial safety factors. The results for the first and second case are summarised in Table 4 and Table 5, respectively.

For the results in both Table 4 and Table 5 the statistical uncertainty of the SN-curve has been disregarded. Otherwise the partial safety product would have

$\beta_t = 3.25$	V_{exp}	V_{aero}	V_{dyn}	V_{stress}	V_{RFC}	V_{SN}	η	FDF	$\gamma_m \gamma_f$
Reference	0.20	0.20	0.10	0.05	0.02	0.05	1	873	2.69
Exposure	0.10	-	-	-	-	-	.86	311	2.32
Aerodyn.	-	0.10	-	-	-	-	do.	do.	do.
Dynamics	-	-	0.05	-	-	-	.965	684	2.60
Exp.+aero	0.10	0.10	-	-	-	-	.71	84	1.91
All three	0.10	0.10	0.05	-	-	-	.665	54	1.79

Table 5: calibrated partial safety factor products for the hub material when statistical uncertainty of the SN-curve is disregarded. The first row gives the reference model uncertainties taken from [4]. In the second to the sixth row a dash means that the reference value given in the first row is used. β_t is given in the upper left corner.

been almost insensitive to the model uncertainties. This follows from the plots in Figure 13 showing virtually no sensitivity of the reliability to the model uncertainties if statistical uncertainty of the SN-curve is included in the uncertainty model. Under all the assumptions made it is seen that considerable amounts of material can be saved – without changing the level of safety – simply by improving the models (the possible relative material reduction is given by $1-\eta$). In order to verify the results obtained it is relevant to investigate in much further detail the proper modelling of model uncertainties, that is the value of the COV as well as the choice of distribution type. This is a subject that has not yet been dealt with to the degree of detail that it deserves because traditionally these uncertainty sources have been considered of less importance than many other sources. This is true for extreme loads in the storm situation but not for fatigue where they *are* of importance. Adding to this that for many components of wind turbines the fatigue loads are design-driving the need for further investigations into the subject of model uncertainties is crucial.

Results involving statistical uncertainties related to the SN-curve are not provided here because there is too little data available in the project to carry out an analysis. E.g. one subject of such an analysis would be the influence of having more test data and test data at other stress levels.

4 Conclusions

In this report examples of fatigue lifetime and reliability evaluation of larger wind turbine components have been given. Part of the investigation has been the discussion of possible uncertainty sources that influences the lifetime distribution and their quantification.

The work being based on three example components and further the probabilistic analysis being simplified the applicability of results and conclusions reached in this report is limited. The results and discussions are however of general qualitative validity.

The major conclusions are:

- That statistical uncertainty of the determination of the SN-curve from limited amounts of test data greatly influences the lifetime distribution if the tests have been carried out at stress levels that are higher than those present in the load history that the material becomes subject to.
- On the other hand statistical uncertainty relating to site-specific assessment of mean wind distribution from at least one year of measurements hardly influences the lifetime distribution.
- Because model uncertainties relating to stresses are raised to the power of the Wöhler exponent the sensitivity of the lifetime to these uncertainties can be quite significant. This correct modelling of the model uncertainties is a subject that has not yet been dealt with to the degree of detail that it deserves because traditionally these uncertainty sources have been considered of less importance than many other sources. This is true for extreme loads in the storm situation but not for fatigue where they *are* of importance. Adding to this that for many components of wind turbines the fatigue loads are design-driving the need for further investigations into the subject of model uncertainties is crucial. Below a recommendation for the future work in this field is given.
- The three components showed to have significantly different levels of safety. As explained in the introduction these differences are expected to result partly from the fact that different manufacturers that have contributed with the design of the components may have different design strategies, partly from the fact that in any turbine not all components are designed fully to the limit. Thus any turbine design has a bottleneck, which then can be one of the components considered herein, i.e. the main shaft. However the safety of the shaft seemed to be very low, implying that other reasons than the bottleneck-argument may exist. These have not been uncovered during the course of the project. The reason that the frame has very high reliability can be that the design strategy implies very conservative assessment of design loads.
- Studies of partial safety factor calibrations show that considerable amounts of material can be saved. However this conclusion rests on the validity of the modelling of the model uncertainty, which is discussed above.

Recommendation for Future Work:

One issue of this report has been the discussion of uncertainty sources. From this discussion it has been learned that the minute one starts to think about uncertainty sources related to the response simulation, the stress range count, and the application of the SN-curve the picture becomes so full of details that it is difficult overview.

It is therefore recommended, as a potentially fruitful approach to assessing some of the contributions to the overall uncertainty of the lifetime, that one invites different engineers to compute the lifetime of a certain component. The different results that would come out of these computations would then account for the distribution of the lifetime uncertainty due to the uncertainties related to the response simulation, the stress range count, the application of the SN-curve, etc.

For the modelling of e.g. the exposure model uncertainty (i.e. the uncertainty relating to the influence of the terrain topology) comparing long-time measurements of the climates at several specific – but typical – sites with WASP computations and/or short-term measurements could give information that could lead to the establishment of a distribution for exposure model uncertainty.

References

- [1] Tarp-Johansen, N.J.: "Notat angående Metodevalg for probabilistisk analyse" (in Danish), May 2001, Wind Energy Department, Risø National Laboratory
- [2] Ditlevsen, O., and H.O. Madsen: "Structural Reliability Methods", Wiley, 1996, ISBN 0-471-96086-1
- [3] Tarp-Johansen, N.J.: "Note: Beskrivelse af statistisk usikkerhed for Weibullparametre fastsat ud fra et års målinger" (in Danish), November 2001, Wind Energy Department, Risø National Laboratory
- [4] Tarp-Johansen, N.J., P.H. Madsen, and S.T. Frandsen: "Background document for Partial Safety Factors for Extreme Load Effects, Proposal for the 3rd Ed. of IEC 61400: Wind Turbine Generator Systems - Part 1: Safety Requirements", Risø report R-1319(EN), Risø National Laboratory, 2003, ISBN 87-550-3002-5
- [5] Wilhelmsen, T.: Reports from the project (PSO 2079, ELSAM)
- [6] Montgomery, D. C.: "Design and Analysis of Experiments", 3rd Ed., Wiley, 1991, ISBN 0-471-52994-X
- [7] Brøndsted, P.: Private communication.

Title and authors

Examples of Fatigue Lifetime and Reliability Evaluation of Larger Wind Turbine Components

Niels Jacob Tarp-Johansen

ISBN	ISSN
87-550-3236-2 (Internet)	0106-2840
Department or group	Date
Wind Energy Department	March 2003
Groups own reg. number(s)	Project/contract No(s)
1120124-00	PSO 2079

Sponsorship

Public Service Obligation

Pages	Tables	Illustrations	References
41	5	17	7

Abstract (max. 2000 characters)

This report is one out of several that constitute the final report on the ELSAM funded PSO project “Vindmøllekomponenters udmattelsesstyrke og levetid”, project no. 2079, which regards the lifetime distribution of larger wind turbine components in a generic turbine that has real life dimensions.

Though it was the initial intention of the project to consider only the distribution of lifetimes the work reported in this document provides also calculations of reliabilities and partial load safety factors under specific assumptions about uncertainty sources, as reliabilities are considered to be of interest to potential readers too.

Descriptors INIS/EDB

FATIGUE; PROBABILISTIC ESTIMATION; RELIABILITY; SERVICE LIFE; WIND TURBINES